Life Sciences 233 (2019) 116631

Contents lists available at ScienceDirect

Life Sciences

journal homepage: www.elsevier.com/locate/lifescie

Calpain silencing alleviates myocardial ischemia-reperfusion injury through the NLRP3/ASC/Caspase-1 axis in mice

Rong-Chuan Yue[a,1], Sheng-Zhong Lu[a,1], Yu Luo[b], Tao Wang[c], Hao Liang[a], Jing Zeng[a], Jie Liu[a], Hou-Xiang Hu[a,*]

[a] Department of Cardiology, Affiliated Hospital of North Sichuan Medical College, Nanchong 637000, PR China
[b] CSSD, Affiliated Hospital of North Sichuan Medical College, Nanchong 637000, PR China
[c] Department of Pathophysiology, North Sichuan Medical College, Nanchong 637000, PR China

ARTICLE INFO

Keywords:
Calpain
NLR pyrin domain containing 3/ASC/Caspase-1
Pyroptosis
Endoplasmic reticulum stress

ABSTRACT

Aims: Prior to reperfusion, Calpains remain inactive due to the acidic pH and elevated ionic strength in the ischemic myocardium; but Calpain is activated during myocardial reperfusion. The underlying mechanism of Calpain activation in the ischemia-reperfusion (I/R) is yet to be determined. Therefore, the present study aims to investigate the mechanism of Calpain in I/R-induced mice.

Main methods: In order to detect the function of Calpain and the NLRP3/ASC/Caspase-1 axis in cardiomyocyte pyroptosis, endoplasmic reticulum (ER) stress and myocardial function, the cardiomyocytes were treated with hypoxia-reoxygenation (H/R), and NLRP3 were silenced, Calpain was overexpressed and Caspase-1 inhibitors were used to determine cardiomyocyte pyroptosis. The results obtained from the cell experiments were then verified with an animal experiment in I/R mice.

Key findings: There was an overexpression in Calpain, ASC, NLRP3, GRP78 and C/EBP homologous protein (CHOP) in cardiomyocytes following H/R. A significant increase was witnessed in lactic acid dehydrogenase (LDH) activity, cardiomyocyte pyroptosis rate, Calpain activity, reactive oxygen species (ROS) concentration, as well as activation of ER stress in cardiomyocytes after H/R. However, opposing results were observed in H/R cardiomyocytes that received siRNA Calpain, siRNA NLRP3 or Caspase-1 inhibitor treatment. Overall, the results obtained from the animal experiment were consistent with the results from the cell experiment.

Significance: The silencing of Calpain suppresses the activation of the NLRP3/ASC/Caspase-1 axis, thus inhibiting ER stress in mice and improving myocardial dysfunction induced by I/R, providing a novel therapeutic pathway for I/R.

1. Introduction

Ischemia/reperfusion (I/R) is the feature of various diseases, including peripheral vascular diseases, myocardial infarction and stroke, remains one of the most common causes of debilitating diseases and death [1]. Myocardial infarction, which has been identified as the leading cause of mortality worldwide, mainly occurring as a result of two conditions: atherosclerosis of the coronary arteries and shortage in blood supply to the heart [2]. However, the specific mechanism of its pathogenesis still remains unclear [3]. Pyroptosis is a host cell death pathway, which has been identified to be stimulated by a group of microbial infections and non-infectious stimuli, including the host factors following myocardial infarction [4]. I/R could potentially result in the activation of apoptotic pathways and acceleration of I/R injury by inducing the unfolded protein response and endoplasmic reticulum (ER) stress [5]. Recent studies have illustrated various therapeutic options that could potentially prevent I/R-induced tissue injury with unspecific local or systemic physical stressors, pharmacological agents, growth factors or all of the aforementioned options [6]. However, the relationship that exists between pyroptosis and I/R injury is yet to be thoroughly investigated. As a result, further studies are required to determine the related influence factors of pyroptosis, ER stress and I/R injury rewired in order to provide a novel therapy for I/R injury.

Calpain 1, a ubiquitous cysteine protease, is present in the cytosol

* Corresponding author at: Department of Cardiology, Affiliated Hospital of North Sichuan Medical College, No. 63, Wenhua Road, Shunqing District, Nanchong 637000, Sichuan Province, PR China.
E-mail address: hhxiang17@163.com (H.-X. Hu).
[1] These authors are regarded as co-first authors.

https://doi.org/10.1016/j.lfs.2019.116631
Received 13 March 2019; Received in revised form 18 June 2019; Accepted 2 July 2019
Available online 03 July 2019

and cardiac mitochondria, and the release of mitochondrial calpain 1 within the intermembrane space results in the elevation of cardiac injury by promoting the production of pro-apoptotic factors from mitochondria during IR [7]. Caspase-1 has been found to be induced in auto-inflammatory disorders, as mutations in the gene encoding nucleotide-binding oligomerization domain-like receptor with a pyrin domain (NLRP) 3 result in the spontaneous activation of Caspase-1, which contributes to a series of NLRP3-related periodic fever syndromes [8]. The production of inflammasomes is large multiprotein complexes consisting of Caspase-1, apoptosis-associated speck-like protein (ASC), and NLRP of cardiac fibroblasts is indispensable for myocardial I/R injury [9,10]. ASC is an important regulator molecule of inflammasomes that could mediate inflammatory and apoptotic signals [11]. Another previously conducted study has demonstrated that the NLRP3-ASC-Caspase-1 inflammasome was considered as a novel innate immune sensor and a powerful pro-inflammatory cytokine [12]. Moreover, both NLRP3 and its downstream target Caspase-1 are overexpressed in I/R and are important for hepatic I/R injury evidenced by NLRP3 and Caspase-1 knockout mice which have been found to be protected from injury [13]. Calpain has been identified as an important proteolytic enzyme in the myocardium [14]. Calpain activation, obtained by binding to calcium might cause the degradation of cell structural proteins, making it a key factor in myocardial dysfunction [15]. In addition, the inhibition of Calpain could potentially be of use as it can limit the infarction size during reperfusion [16]. In addition, it has been reported that Calpain inhibition could potentially prevent or attenuate myocardial injury during I/R, and advanced myocardial infarction [17]. However, the underlying mechanisms by which Calpain aggravates I/R remain unknown. Therefore, the present study was conducted with the main objective of exploring the association between Calpain and I/R injury, in order to propose a novel therapeutic pathway for I/R injury.

2. Materials and methods

2.1. Ethical statements

This study was carried out with strict accordance with the recommendations in the Guidelines for the Care and Use of Laboratory Animals of the National Institutes of Health. The experiments were carried out with the approval of the committee of North Sichuan Medical College.

2.2. Cell culture and treatment

The hypoxia-reoxygenation (H/R) model was induced using cardiomyocytes of C57BL/6 mice (No. M6200, Shanghai Zhongqiaoxinzhou Biotechnology Co., Ltd., Shanghai, China). The 24-well cell culture plate was placed in a gas mixture containing 1% O_2, 5% CO_2 and 94% N_2. After 24 h of hypoxia culture, the cardiomyocytes were restored to 21% O_2, 5% CO_2 and 74% N_2 for reoxygenation [18].

2.3. Cell grouping

The cardiomyocytes were treated in accordance with the requirements of each group. All plasmids were purchased from Genechem (Shanghai Genechem Co., Ltd., Shanghai, China) and the concentration was 10 mM. Once the H/R treatment was completed, the morphological changes of cardiomyocytes were observed under an inverted microscope. Except for the normal cardiomyocytes, H/R cardiomyocytes received treatment with PBS, z-VAD-FKM, si-NC, si-NLRP3, tunicamycin (TM), 4-phenyl butyric acid (4-PBA), pcDNA control, pcDNA Calpain, si-Calpain, pcDNA Calpain + z-VAD-FKM, pcDNA Calpain + si-NLRP3, and pcDNA Calpain + 4-PBA or were left without any treatment. The transfection was carried out with the use of the Lipofectamin 2000 kit (11668019; Thermo Fisher Scientific Inc., Waltham, MA, USA). A total of 4.5 μL plasmid was cultured with 1.5 μL Lipofectamin 2000 for 48 h. The cells that had undergone different treatments were then incubated with 10 μmol/L Capase-1 inhibitor, 100 ng/mL ER stress agonist TM and 5 μmol/mL ER stress inhibitor 4-PBA for 6 h. Afterwards, H/R treatment was carried out.

2.4. Reverse transcription quantitative polymerase chain reaction (RT-qPCR)

Trizol reagents (No. 16096020, Thermo Fisher Scientific Inc., Waltham, MA, USA) were used for the extraction of the total RNA in the tissues or cells. A total of 5 μg total RNA was reversely transcribed into cDNA according to the instructions provided on the RT-qPCR Kit (ABI, Oyster Bay, NY, USA). The PROGENE PCR amplification instrument (Techene Ltd., Cambridge, UK) was used for the amplification of the target gene in the 25 μL system which included 300 ng cDNA, 1 × PCR buffer, 200 μmol/L deoxyribonucleotide triphosphates (dNTPs), forward and reverse primers (80 pmol/L each) and 0.5 U Taq enzyme (S10118, Shanghai Yuanye Biotechnology Co., Ltd., Shanghai, China). The reaction conditions were as follows: pre-denaturation at 94 °C for 5 min, 30 cycles of denaturation at 94 °C for 30 s, annealing at 54.5 °C for 30 s and extension at 72 °C for 30 s, and a final extension at 72 °C for 10 min. The samples were finally stored at 4 °C. The primer sequences of NLRP3, ASC, Caspase-1, 78-kDa glucose-regulated protein (GRP78), C/EBP homologous protein (CHOP), Calpain and glyceraldehyde-3-phosphate dehydrogenase (GAPDH) are displayed in Table 1. GAPDH was considered as the internal reference of the genes. The expression of target genes was calculated based on the $2^{-\Delta\Delta Ct}$ method, with ΔCt obtained using the following formula: ΔCt = Ct (target gene) − Ct (GAPDH), and ΔΔCt = ΔCt (the experiment group) − ΔCt (the control group). The experiment was conducted in triplicates.

2.5. Western blot analysis

Following transfection, the cells in each group were lysed with radio immunoprecipitation assay (RIPA) lysis buffer (P0013B, Beyotime biotechnology, Shanghai, China), and the total protein content of the cells were detected with the use of bicinchoninic acid (BCA) kit. A total of 50 μg protein was dissolved in 2 × sodium dodecyl sulfate (SDS) loading buffer and boiled at 100 °C for 5 min. Subsequently, the above samples were separated using the 10% SDS-polyacrylamide gel electrophoresis (SDS-PAGE), transferred onto a polyvinylidene fluoride (PVDF) membrane using the wet transfer method, and blocked with the 5% skimmed milk powder at room temperature for 1 h. Subsequently, the PVDF membrane was incubated with the primary antibodies, polyclonal rabbit antibodies against NLRP3 (1:1000, ab214181), ASC (1:1000, ab47092), Caspase-1 (1:2000, ab138483), GRP78 (1:1000, ab21685), CHOP (1:800, ab10444) and Calpain (1:1000, ab28258) and monoclonal mouse antibody against GAPDH (1:10000, ab181602)

Table 1
Primer sequences for RT-qPCR.

Sequences	Forward (5′-3′)	Reverse (5′-3′)
NLRP3	CCAGGGCTCTGTTCATTG	CCTTGGCTTTCACTTCG
ASC	CCCATAGACCTCACTGATAAAC	AGAGCATCCAGCAAACCA
caspase-1	AGGAGGGAATATGTGGG	AACCTTGGGCTTGTCTT
GRP78	CTACCGGGACGAGGTACTGG	GGAAAAGGCGGTGAGGACTT
CHOP	CGGAGTGTACCCAGCACCATCA	CCCTCTCCTTTGGTCTACCCTCA
Calpain	CTACGAGGTTCCCAAAGAGATG	CCCGCATGTTGATGTAGGT
GAPDH	AGTGCCAGCCTCGTCTCATAG	CCTTGACTGTGCCGTTGAACT

Notes: RT-qPCR, reverse transcription quantitative polymerase chain reaction; NLRP3, NLR pyrin domain containing 3; ASC, apoptosis-associated speck-like protein containing a caspase recruitment domain; GRP78, 78-kDa glucose-regulated protein; CHOP, C/EBP homologous protein; GAPDH, glyceraldehyde-3-phosphate dehydrogenase.

overnight. The membrane underwent incubation with horseradish peroxidase (HRP)-labeled secondary antibody (1:5000) for 1 h after being washed 3 times with tris-buffered saline tween (TBST) solution (Boster Biological Technology Co., Ltd., Wuhan, Hubei, China). All of the aforementioned antibodies were purchased from Abcam (Cambridge, MA, USA). The solution A and solution B from a chemiluminescence (ECL) fluorescent detection kit (BB-3501, Amersham Pharmacia, Piscataway, NJ, USA) was mixed under dark conditions, after which it was dripped onto the membranes and exposed in the gel imager. The images were visualized using a Bio-Rad image analysis system (Bio-Rad Laboratories, Hercules, CA, USA). The ratio of the gray value of the target protein band to that of the β-actin protein band was obtained using the Quantity One v4.6.2 software in order to determine the relative protein levels. The experiment was conducted in triplicates.

2.6. Detection of lactic acid dehydrogenase (LDH) activity, ROS content and Calpain activity

LDH activity detection: the cells were collected in a 96-well plate, followed by the addition of 200 μL medium to each well, with blank medium used as the control. Three replicates were set in each group [19].

ROS content detection: the cells and heart tissues were collected following transfection, and the ROS content was detected according to the references [20, 21].

Calpain activity detection: a total of 1–2 × 10^6 cells or about 0.1 g tissues were collected for the detection, and the activity of Calpain was detected using a procedure performed in previous studies [22,23]. The above experiments were conducted in triplicates.

2.7. Propidium iodide (PI)/Hoechst 33342 double staining

The cells from each group were collected following treatment with 0.125% trypsin. Next, the PI and Hoechst 33342 were added to the collected cells for double staining for 10 min. Then, the cells were observed and photographed under an inverted fluorescence microscope (Carl Zeiss, Oberkochen, Germany). If the PI could penetrate the pyroptosis cell membrane and enter into the nucleus, which was determined by the appearance of a red fluorescence, indicating the presence of dead cells as a result of pyroptosis. The pyroptosis rate was calculated using the formula: pyroptosis rate = the dead cell number/the total cell numbers × 100%. The experiment was conducted in triplicates to obtain the mean value.

2.8. Trypan blue staining

Cells in the logarithmic growth phase were treated with 0.25% trypsin. Next, cell suspension and 4% trypan blue solution were mixed at the ratio of 9:1 (v/v). The terminal concentration of trypan blue was 0.4%. Until the adherent cells dropped, the living cells (non-staining) and dead cells (blue staining) were counted with a cell counting plate, and the cell survival rate was calculated using the following formula: cell survival rate (%) = the number of living cells/(the number of living + dead cells) × 100%. The experiment was conducted in triplicates in each group [24].

2.9. Animal grouping

A total of 163 male C57BL/6 mice (aged 2–4 month; weighing 20 ± 4 g) were provided by Laboratory Animal Center of North Sichuan Medical College (Nanchong, Sichuan, China). I/R mice were pre-treated with PBS, z-VAD-FKM, si-NC, si-NLRP3, TM, 4-PBA, pcDNA control, pcDNA Calpain, si-Calpain, pcDNA Calpain + z-VAD-FKM, pcDNA Calpain + si-NLRP3, and pcDNA Calpain + 4-PBA or were left without any treatment; there were 10 mice in the normal group and the sham group separately, while there were 11 mice in the remaining groups. The mice were pretreated according to the requirements 30 min prior to ischemia. The normal mice were raised without receiving any treatment. For sham-operated mice, after the administration of anesthesia, throracotomy was conducted and the mice were threaded without ligation. The mice that had undergone I/R treatment were initially injected with adeno-associated virus 9 (AAV9) vectors carrying plasmids intravenously or z-VAD-FKM (1.5 mg/kg), TM (0.6 mg/kg) intraperitoneally or administrated with 4-PBA (1 g/kg) intragastrically. After 30 min, the mice were ligated for 45 min to induce ischemia and subjected to reperfusion for 3 h.

2.10. Model establishment

The mouse model with myocardial I/R injury was established through the ligation/release method of the left anterior descending coronary artery (LAD) [24]. The indexes of the samples were detected after 3 h of reperfusion. The success rate of induction was 79.08% (121/153) with 121 successfully established I/R mouse models and about 1–4 dead mice in each group, except for the normal group.

2.11. Detection of cardiac function indexes

The left ventricle was connected to the pressure transducer (Maclab/4S) with cannula to detect cardiac function index/indicator continuously through the connection of Maclab/4S analog converter (AD Struments, New South Wales, Australia) and macho-sh7200/90-type computer (Apple Computer Inc., Cupertino, CA, USA). After 3 h, three mice were selected from each group and subjected to thoracic surgery. Subsequently, a small opening was made on the left atrial appendage of the mice, and a piezometer tube was inserted with small latex water sac into the left ventricle through the mitral orifice. Then the tube was connected to the pressure transducer, which could mediate the volume of water sac in the left ventricle to adjust the left ventricular end diastolic pressure (LVEDP) into 4–6 mmHg by connecting to the three-way aqueous syringe. The macintosh 7200/90 microcomputer was used to record the left ventricular function indexes in real-time including the LVEDP, left ventricular systolic pressure (LVSP), the maximal rate of rise of the left ventricular pressure ($+dp/dt_{max}$), the maximal rate of fall of the left ventricular pressure($-dp/dt_{max}$), heart rate (HR), and coronary flow (CF).

2.12. Evans blue and 2,3,5-triphenyl tetrazolium chloride (TTC) double staining

Three hours after the completion of the previous experiment, four mice were selected from each group for thoracic surgery, with the LAD ligated again through the retrograde infusion of 1% evens blue from the carotid artery in order to determine whether the myocardium was ischemic or non-ischemic (the non-ischemic myocardium presented with blue staining, while the ischemic myocardium were not stained). After the mice were euthanized through the injection of 10% KCl, the heart was extracted from the mice. Following the removal of the cardiac base, heart atrium and right ventricle, the left ventricle was weighed, and evenly divided into 4 segments from the cardiac apex to the cardiac base. The slices were incubated with 1% freshly prepared TTC solution for 15 min at 37 °C to distinguish the infarct and non-infarct sizes (the infarct size was not stained, while the non-infarct size was stained in red). The slices were photographed using a digital camera, followed by the analysis using Sigma Scan Pro v4.0 (Systat Software Inc., Point Richmond, CA, USA) to calculate the ratio of myocardial infarction size [25].

2.13. Transmission electron microscope (TEM) observation

The anterior wall tissue blocks (1 mm × 1 mm × 1 mm) of mouse left ventricle were fixed in 2.5% glutaraldehyde solution at 4 °C for 4 h.

Subsequently, the samples were rinsed 4 times with 0.1 mol/L PBS (each for 15 min), and fixed in 1% osmic acid solution at 4 °C for 2 h. The tissue blocks underwent dehydration with 50%, 70%, 90% and 100% gradient acetone (each for 15 min), and received treatment with the mixture of 100% acetone and resin at the ratio of 1:1 for 2 h and the mixture of 100% acetone and resin at the ratio of 1:2 for additional 2 h, followed by absolute resin penetration overnight. Afterwards, the tissues were embedded with Epon 812 resin, polymerized at 37 °C for 12 h, at 45 °C for 12 h, and at 60 °C for 48 h. The samples were sliced into ultrathin sections (60–70 nm), stained with uranyl acetate and lead nitrate, and observed under a TEM (Tecnai G2 Spirit Bio TWIN, Thermo Fisher Scientific, Waltham, MA, USA). The experiment was conducted in triplicates.

2.14. Statistical analysis

Statistical analyses were conducted by using SPSS 21.0 (IBM, Armonk, NY, USA). The measurement data were expressed as mean ± standard deviation. The data were first tested for normality distribution and homogeneity of variance. If data conform to normality distribution and had homogeneity of variance, the difference between two groups was compared by unpaired *t*-test, while multiple groups were compared by one-way analysis of variance (ANOVA). If the data did not conform to normal distribution or homogeneity of variance, they were tested by the rank-sum test. $p < 0.05$ was considered statistically significant.

3. Results

3.1. H/R induces cardiomyocyte pyroptosis

In order to investigate the effect of H/R on the pyroptosis of cardiomyocytes, the H/R cell models were established in vitro and pyroptosis of cardiomyocytes was detected in both the normal and H/R groups. The results from RT-qPCR and western blot analysis revealed that levels of Calpain, the inflammasome NLRP3, and ER stress-related genes GRP78 and CHOP were significantly higher in the H/R group than those in the normal group (all $p < 0.05$; Supplementary Fig. 1A–C). Pyroptosis and cell survival rates as well as LDH concentration determination showed that there was a significant increase in cardiomyocyte pyroptosis rate and LDH concentration, while the cell survival rate was significantly decreased in the H/R group relative to the normal group ($p < 0.05$). The Calpain activity and ROS content detections showed a significant increase in Calpain activity in cardiomyocytes and ROS content in the H/R group when compared with the normal group ($p < 0.05$; Supplementary Fig. 1D–I). These results suggest that H/R could induce cardiomyocyte pyroptosis.

3.2. ER stress potentiates H/R-induced cardiomyocyte pyroptosis

ER stress agonist TM and inhibitor 4-PBA were added in vitro in order to investigate the effect of ER stress on cardiomyocyte pyroptosis induced by H/R. Based on the results of RT-qPCR and western blot analysis, there was no significant difference in the expression of GRP78 and CHOP in the PBS + H/R group in comparison with the H/R group ($p > 0.05$); the expression of GRP78 and CHOP was significantly increased in the TM + H/R group and decreased in the 4-PBA + H/R group ($p < 0.05$). The ROS content detection showed in comparison with the H/R group, there was no significant difference in ROS content in the PBS + H/R group ($p > 0.05$); the ROS content was significantly increased in the TM + H/R group, while it was decreased in the 4-PBA + H/R group ($p < 0.05$; Fig. 1A–C).

The detection of pyroptosis and cell survival rates revealed that compared with the H/R group, there was no significant difference in cardiomyocyte pyroptosis rate and cell survival rate in the PBS + H/R group ($p > 0.05$); there was a significant increase in the cardiomyocyte pyroptosis rate, while the cell survival rate was significantly decreased in the TM + H/R group; the cardiomyocyte pyroptosis rate was significantly decreased and the cell survival rate was significantly increased in the 4-PBA + H/R group ($p < 0.05$). The detection of LDH concentration revealed that compared with the H/R group, there was no significant difference in the LDH concentration in the PBS + H/R group ($p > 0.05$). Compared with the H/R group, there was a remarkable increase in the LDH content of myocardial cells in the TM + H/R group ($p < 0.05$), while it was significantly decreased in the 4-PBA + H/R group ($p < 0.05$; Fig. 1D–H). These findings suggested that ER stress could potentially induce cardiomyocyte pyroptosis.

3.3. Caspase-1 results in H/R-induced cardiomyocyte pyroptosis

Furthermore, in order to investigate whether Capase-1 has an effect on the pyroptosis of cardiomyocytes after H/R, we added the inhibitor of Capase-1 for further exploration. Based on the results from RT-qPCR and western blot analysis, there was no significant difference in GRP78 and CHOP expression in cardiomyocytes of the PBS + H/R group in comparison with the H/R group ($p > 0.05$), while the GRP78 and CHOP expression significantly decreased in the z-VAD-FKM + H/R group ($p < 0.05$). The ROS content was detected and the results revealed that compared with the H/R group, there was no significant difference in ROS content in cardiomyocytes of the PBS + H/R group ($p > 0.05$); ROS content was significantly decreased in the z-VAD-FKM + H/R group ($p < 0.05$; Fig. 2A–D).

Pyroptosis and cell survival rate were detected and the findings showed that compared with the H/R group, there was no significant difference in cardiomyocyte pyroptosis rate and cell survival rate of the PBS + H/R group ($p > 0.05$); in the z-VAD-FKM + H/R group, there was a significant decrease in the cardiomyocyte pyroptosis rate, while the cell survival rate was significantly increased ($p < 0.05$). After the detection of LDH concentration, the findings showed that compared with the H/R group, there was no significant difference in the LDH concentration of cardiomyocytes of the PBS + H/R group ($p > 0.05$); in the z-VAD-FKM + H/R group, there was a significant decrease in the LDH content in cardiomyocytes ($p < 0.05$; Fig. 2E–H). These findings suggested that Caspase-1 could potentially induce cardiomyocyte pyroptosis.

3.4. NLRP3 inflammasome leads to H/R-induced cardiomyocyte pyroptosis

The effect of NLRP3 inflammasome on the pyroptosis of cardiomyocytes exposed to H/R was evaluated by the downregulation of NLRP3 expression in cardiomyocytes. Following RT-qPCR and western blot analysis, it was found that there was no significant difference in the expression of all factors in the si-NC + H/R group compared with the H/R group ($p > 0.05$); but in cardiomyocytes of the si-NLRP3 + H/R group, there was a decrease in the expression of NLRP3, ASC, Caspase-1, GRP78 and CHOP ($p < 0.05$). Once ROS content was detected, the results showed that there was no significant difference in ROS content in cardiomyocytes of the si-NC + H/R group in comparison with the H/R group ($p > 0.05$); the cardiomyocytes in the si-NLRP3 + H/R group presented with significantly decreased ROS content ($p < 0.05$; Fig. 3A–D).

The detection of pyroptosis and cell survival rates showed that compared with the H/R group, there was no significant difference in cardiomyocyte pyroptosis rate and cell survival rate in the si-NC + H/R group ($p > 0.05$), while the cardiomyocyte pyroptosis rate was significantly decreased and cell survival rate was significantly increased in the si-NLRP3 + H/R group ($p < 0.05$). The LDH concentration was detected and the results showed that compared with the H/R group, there was no significant difference in the LDH concentration of cardiomyocytes in the si-NC + H/R group ($p > 0.05$); in the si-NLRP3 + H/R group, the LDH concentration of cardiomyocytes was significantly

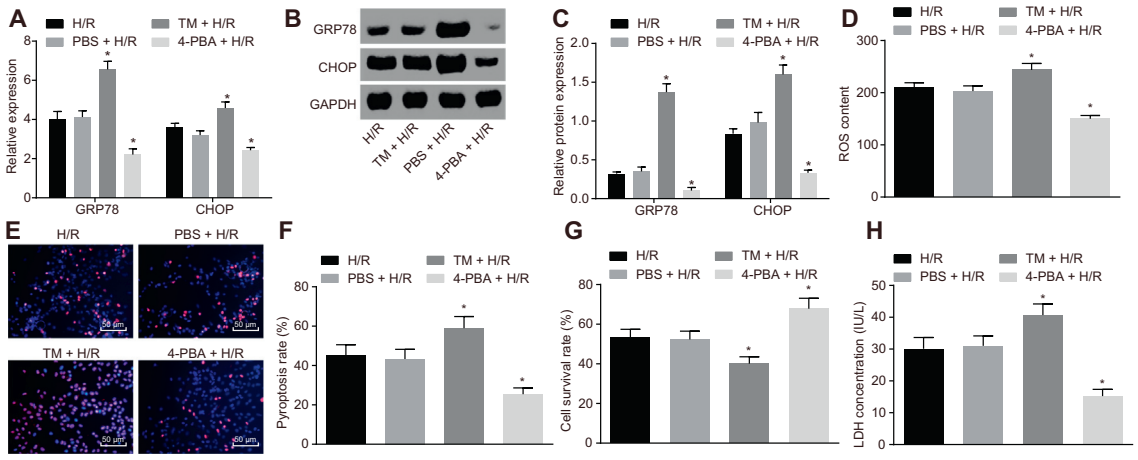

Fig. 1. ER stress promotes H/R-induced cardiomyocyte pyroptosis. The cardiomyocytes were treated with TM, PBS, or 4-PBA combined with H/R or H/R alone. A, the mRNA expression of GRP78 and CHOP; B–C, the protein expression of GRP78 and CHOP; D, the fluorescent staining results of the ROS content in cardiomyocytes; E–F, the PI/Hoechst 33342 double staining results of cardiomyocyte pyroptosis (200 ×); G, the cell survival rate in each group assessed by the trypan blue staining; H, the LDH concentration in cardiomyocyte in each group. The measurement data were expressed in mean ± standard deviation; difference among groups was compared by one-way analysis of variance, followed by Tuckey's post hoc test; the experiment was conducted 3 times; *, $p < 0.05$ vs. the H/R group.

decreased ($p < 0.05$; Fig. 3E–H). Therefore, NLRP3 could potentially induce cardiomyocyte pyroptosis.

3.5. Calpain promotes H/R-induced cardiomyocyte pyroptosis through the NLRP3/ASC/Caspase-1 axis

The effect of Calpain on the pyroptosis of cardiomyocytes after H/R was further investigated through the knockdown or overexpression of Calpain in cardiomyocytes. RT-qPCR and western blot analysis revealed that there was no significant difference in the expression of Calpain, NLRP3, ASC, Caspase-1, GRP78 and CHOP in cardiomyocytes of the pcDNA control + H/R group compared with the H/R group ($p > 0.05$); there was a significant increase in the expression of these factors in the pcDNA Calpain + H/R group ($p < 0.05$), which was observed to have significantly diminished in the si-Calpain + H/R group ($p < 0.05$). The Calpain activity and ROS content detections showed that compared with the H/R group, there was no significant difference in Calpain activity and ROS content in cardiomyocytes of the si-NC + H/R group ($p > 0.05$); the Calpain activity and ROS content in cardiomyocytes of the pcDNA Calpain + H/R group were significantly elevated ($p < 0.05$); the Calpain activity and ROS content in cardiomyocytes of the si-Calpain + H/R group were significantly reduced ($p < 0.05$; Fig. 4A–E).

The detection of pyroptosis and cell survival rates showed that compared with the pcDNA control + H/R group, the cardiomyocyte pyroptosis rate was increased, while the cell survival rate was significantly decreased in the pcDNA Calpain + H/R, pcDNA Calpain + z-VAD-FKM + H/R, pcDNA Calpain + si-NLRP3 + H/R and pcDNA Calpain + 4-PBA + H/R groups, among which the pcDNA Calpain + H/R group presented with the highest cardiomyocyte pyroptosis rate and the lowest cell survival rate (all $p < 0.05$); however, in the si-Calpain + H/R group, the cardiomyocyte pyroptosis rate was significantly decreased and the cell survival rate was significantly increased ($p < 0.05$). The detection of LDH concentration showed that compared with the pcDNA control + H/R group, increased LDH concentration was observed in the pcDNA Calpain + H/R, pcDNA Calpain + z-VAD-

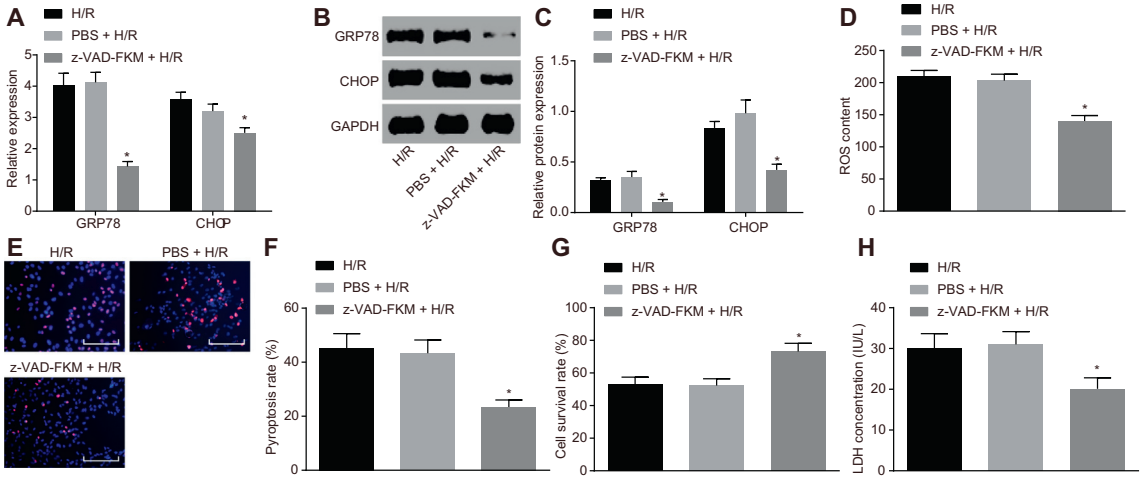

Fig. 2. Caspase-1 activity promotes H/R-induced cardiomyocyte pyroptosis. The cardiomyocytes were treated with PBS or z-VAD-FKM combined with H/R or H/R alone. A, the mRNA expression of GRP78 and CHOP; B–C, the protein expression of GRP78 and CHOP; D, the fluorescent staining results of ROS content in cardiomyocytes; E–F, the PI/Hoechst 33342 double staining results of cardiomyocyte pyroptosis (200 ×); G, the cell survival rate in each group assessed by the trypan blue staining; H, the LDH concentration in cardiomyocyte in each group; the measurement data were expressed with the mean ± standard deviation; difference among groups was compared by one-way analysis of variance, followed by Tuckey's post hoc test; the experiment was conducted 3 times; *, $p < 0.05$ vs. the H/R group.

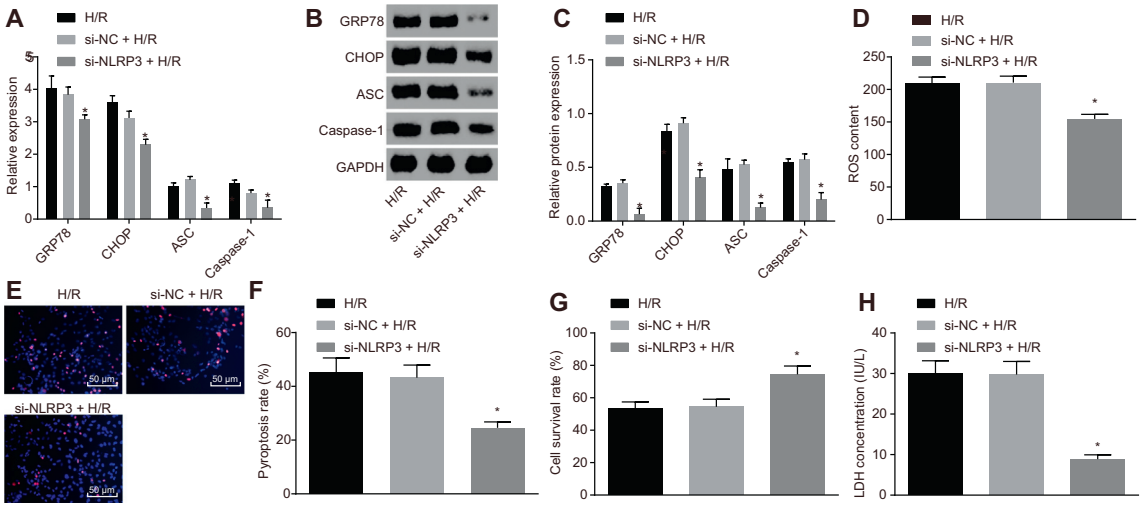

Fig. 3. NLRP3 promotes H/R-induced cardiomyocyte pyroptosis. The cardiomyocytes were treated with si-NC or si-NLRP3 combined with H/R or H/R alone. A, the mRNA expression of GRP78, CHOP, ASC and Caspase-1; B–C, the protein expression of ASC, GRP78, CHOP and Caspase-1; D, the fluorescent staining results of the ROS content in cardiomyocytes; E–F, the PI/Hoechst 33342 double staining results of cardiomyocyte pyroptosis (200×); G, the cell survival rate assessed by the trypan blue staining; H, the LDH concentration in cardiomyocytes; the measurement data were expressed with the mean ± standard deviation; difference among groups was compared by one-way analysis of variance, followed by Tuckey's post hoc test; the experiment was conducted 3 times;*, $p < 0.05$ vs. the H/R group.

FKM + H/R, pcDNA Calpain + si-NLRP3 + H/R and pcDNA Calpain + 4-PBA + H/R groups, among which the pcDNA Calpain + H/R group had the highest LDH concentration (all $p < 0.05$); while in the si-Calpain + H/R group, significantly decreased LDH concentration in cardiomyocytes can be found ($p < 0.05$; Fig. 4F–I). From the aforementioned results, we conclude that Calpain could induce cardiomyocyte pyroptosis through the NLRP3/ASC/Caspase-1 axis.

3.6. I/R induces cardiomyocyte pyroptosis and cardiac function injury in mice

After the I/R model was induced, the myocardial function of the mice was measured. The results showed that compared with the normal group, there was no significant difference in the LVEDP, LVSP, $+dp/dt_{max}$, $-dp/dt_{max}$, HR and CF values in mice in the sham group ($p > 0.05$), while the LVEDP, HR and CF values in mice was significantly increased and the LVSP, $+ dp/dt_{max}$ and $-dp/dt_{max}$ values were significantly decreased in the I/R group ($p < 0.05$; Table 2).

The results from RT-qPCR and western blot analysis revealed that

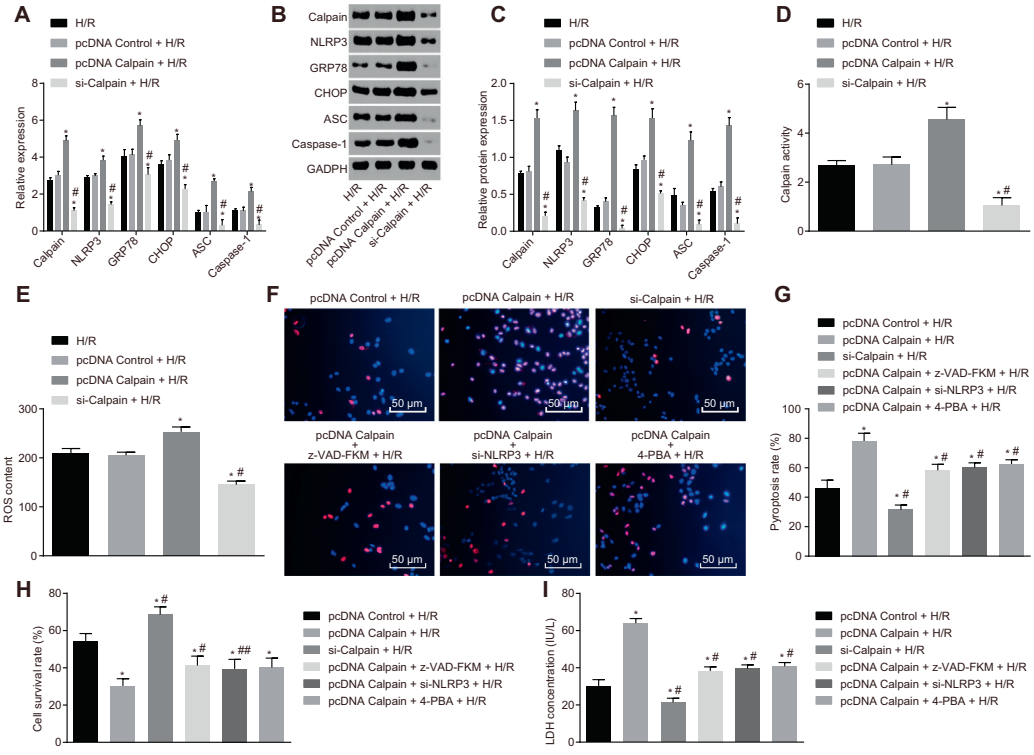

Fig. 4. Calpain enhances H/R-induced cardiomyocyte pyroptosis. The cardiomyocytes were treated with pcDNA Control, pcDNA Calpain or si-Calpain combined with H/R or H/R alone. A, the mRNA expression of Calpain, NLRP3, GRP78, CHOP, ASC and Caspase-1; B–C, the protein expression of Calpain, NLRP3, ASC, GRP78, CHOP and Caspase-1; D, the Calpain activity in cardiomyocytes; E, the fluorescent staining results of the ROS content in cardiomyocytes. The cardiomyocytes were treated with pcDNA control, pcDNA Calpain, si-Calpain, pcDNA Calpain plus z-VAD-FKM, si-NLRP3, or 4-PBA in combined with H/R. F-G, the PI/Hoechst 33342 double staining results of cardiomyocyte pyroptosis (200×); H, the cell survival rate assessed by the trypan blue staining; I, the LDH concentration in cardiomyocytes; the measurement data were expressed with the mean ± standard deviation; difference among groups was compared by one-way analysis of variance, followed by Tuckey's post hoc test; the experiment was conducted 3 times; *, $p < 0.05$ vs. the H/R group or pcDNA control + H/R group; #, $p < 0.05$ vs. the pcDNA Calpain + H/R group.

Table 2
The myocardiac function indexes of mice after I/R.

Group	LVSP (mmHg)	LVEDP (mmHg)	$+dp/dt_{max}$ (mmHg/s)	$-dp/dt_{max}$ (mmHg/s)	HR (times/min)	CF (mL/min)
Normal	120.54 ± 9.86	3.48 ± 1.15	5426.17 ± 648.74	5358.49 ± 654.82	392.67 ± 11.02	9.32 ± 0.89
Sham	126.54 ± 10.12	3.72 ± 1.26	5346.43 ± 628.15	5284.17 ± 641.16	385.33 ± 15.50	9.24 ± 1.51
I/R	92.15 ± 8.26*	11.38 ± 2.54*	3572.84 ± 554.28*	3418.46 ± 547.26*	276.67 ± 20.31*	3.57 ± 0.43*

Notes: LVSP, left ventricular systolic pressure; LVDEP, left ventricular end diastolic pressure; $+dp/dt_{max}$, the maximal rate of rise of the left ventricular pressure; $-dp/dt_{max}$, the maximal rate of fall of the left ventricular pressure; HR, heart rate; CF, coronary flow; I/R, Ischemia-reperfusion. The measurement data (data in table) were expressed with the mean ± standard deviation; difference among groups was compared by one-way analysis of variance, followed by Turkeys' post hoc test.

* $p < 0.05$ vs. the normal group; n = 3.

there was no significant difference in the expression of various factors in mice cardiomyocytes of the sham group compared with the normal group ($p > 0.05$), while the expression of Calpain, NLRP3, GRP78 and CHOP in the I/R group was significantly increased (all $p < 0.05$). Calpain activity was detected and the results showed that there were no significant differences in Calpain activity in cardiomyocytes of the sham group when compared with the normal group ($p > 0.05$), while the Calpain activity was significantly increased in the I/R group ($p < 0.05$; Supplementary Fig. 2A–D).

The detection pyroptosis rate showed that compared with the normal group, there was no significant difference in the pyroptosis rate in mice cardiomyocytes of the sham group ($p > 0.05$), while the pyroptosis rate in mice cardiomyocytes of the I/R group was significantly increased ($p < 0.05$). The results from TEM and TTC/Evans blue staining revealed that the cardiomyocytes of the mice in the normal group presented with a clear cell ultrastructure, regularly arranged mitochondrial cristae and myofilament structure, and there was no evident cell injury or infarction region. Compared with the normal group, there was no significant difference observed in the cell ultrastructure and infarction size of cardiomyocytes in the sham group ($p > 0.05$); in the I/R group of mice cardiomyocytes, local injury was observed in the cells, while partial ER dilated into vacuolization, mitochondrion swelled, partial mitochondrion crest dissolved and myocardial infarction size were all significantly increased (all $p < 0.05$; Supplementary Fig. 2E–I). I/R is considered to induce cardiomyocyte pyroptosis in mice.

3.7. ER stress induces cardiomyocyte pyroptosis and myocardial infarction in I/R mice

In order to study the effect of ER stress on myocardial function of the I/R mice, the ER stress agonist TM and the inhibitor 4-PBA were added in vivo, respectively. The results from RT-qPCR and western blot analysis showed that there was no significant difference observed in the expression of each factor in cardiomyocytes in the PBS + I/R group in comparison with the I/R group ($p > 0.05$), while there was an evident increase in the expression of GRP7 and CHOP in the TM + I/R group and a significant decrease in the expression of GRP78 and CHOP in the 4-PBA + I/R group ($p < 0.05$; Fig. 5A–D).

The pyroptosis rate was detected and the results revealed that there was no significant difference in the cardiomyocyte pyroptosis rate in mice of the PBS + I/R group compared with the I/R group ($p > 0.05$); however, there was a remarkable increase in cardiomyocyte pyroptosis rate in the mice in the TM + I/R group ($p < 0.05$), while the cardiomyocyte pyroptosis rate was significantly decreased in mice of the 4-PBA + I/R group ($p < 0.05$). The results from TEM and TTC/Evans blue staining showed that compared with the I/R group, there was no significant difference in the cell ultrastructure and myocardial infarction size in mice of the PBS + I/R group ($p > 0.05$); in the TM + I/R group of mice, severe cardiomyocyte injury was observed with a disorderly arranged myofilament, dissolution of the focal myofilament, breakage in majority of the mitochondria, swelling of the ER, and a significant increase in the myocardial infarction size. The mice in the 4-PBA + I/R group presented with alleviated cardiomyocyte injury, the ER appeared to have no dilatation, there was occasional vacuolization in mitochondria, and the myocardial infarction size was significantly decreased (all $p < 0.05$; Fig. 5E–I). The cardiac function detection results showed that compared with the I/R group, there was no significant difference in the cardiac function indexes of the PBS + I/R group ($p > 0.05$); in the TM + I/R group, the LVEDP value was significantly increased ($p < 0.05$), while the LVSP, HR, CF, $+dp/dt_{max}$ and $-dp/dt_{max}$ values were significantly decreased ($p < 0.05$); in the 4-PBA + I/R group, the LVEDP value was significantly reduced ($p < 0.05$), while the LVSP, HR, CF, and the $+dp/dt_{max}$, $-dp/dt_{max}$ values were significantly enhanced ($p < 0.05$; Table 3). These findings indicated that ER stress could potentially promote cardiomyocyte pyroptosis, myocardial infarction and cardiac function injury in mice.

3.8. Caspase-1 induces cardiomyocyte pyroptosis and further promotes myocardial infarction and cardiac function injury in I/R mice

Next, Caspase-1 inhibitor was added to detect whether Caspase-1 has an effect on myocardial function in I/R mice. The results from RT-qPCR and western blot analysis showed that compared with the I/R group, there was no significant difference observed in the expression of each factor in the PBS + I/R group ($p > 0.05$); however, there was a significant decrease in the expression of GRP78 and CHOP in the z-VAD-FKM + I/R group (all $p < 0.05$; Fig. 6A–C).

The detection of pyroptosis rate showed that compared with the I/R group, there was no significant difference in the cardiomyocyte pyroptosis rate of the PBS + I/R group ($p > 0.05$); while the cardiomyocyte pyroptosis rate in the z-VAD-FKM + I/R group was significantly decreased (all $p < 0.05$). The results from TEM and TTC/Evans blue staining showed that compared with the I/R group, there was no significant difference in the cell ultrastructure and myocardial infarction size of the PBS + H/R group of mice ($p > 0.05$); in the z-VAD-FKM + I/R group, the extent of cardiomyocyte injury was decreased, along with a decrease in ER dilation and occasional vacuolization in the mitochondria, and myocardial infarction size was significantly smaller (all $p < 0.05$; Fig. 6D–H). The myocardial function detection results showed that compared with the I/R group, there was no significant difference observed in cardiac function indexes in the PBS + I/R group ($p > 0.05$); in the z-VAD-FKM + I/R group, the LVEDP value in mice was significantly decreased ($p < 0.05$), the LVSP, HR, CF, $+dp/dt_{max}$, $-dp/dt_{max}$ values in mice were significantly increased ($p < 0.05$; Table 4). These results are indicative of the ability of Caspase-1 in inducing cardiomyocyte pyroptosis, further promoting myocardial infarction and cardiac function injury in I/R mice.

3.9. NLRP3 enhances cardiomyocyte pyroptosis and further promotes myocardial infarction and myocardial function injury in I/R mice

The expression of NLRP3 was silenced in vivo in order to determine its impact on myocardial function in I/R mice. The results from RT-qPCR and western blot analysis showed that compared with the I/R group, there was no significant difference in the expression of each

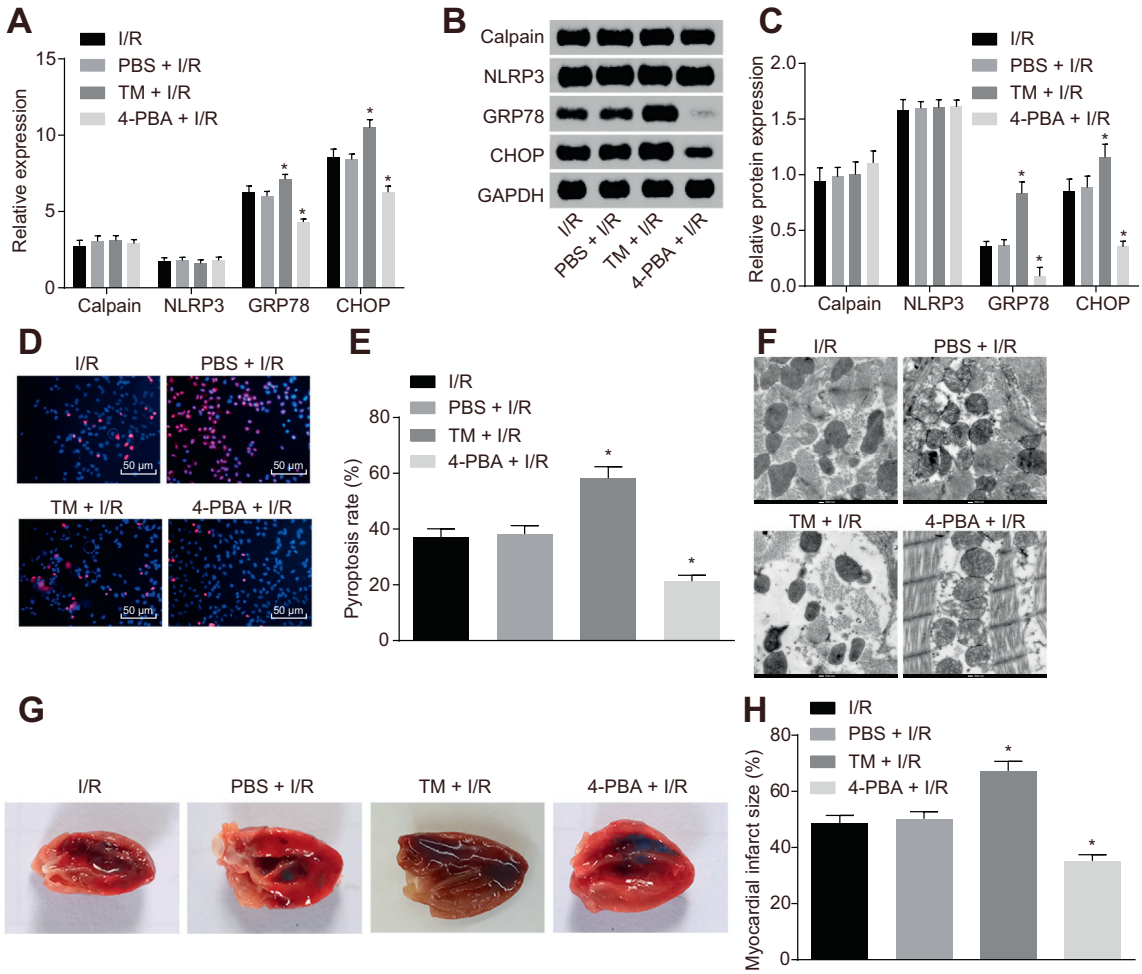

Fig. 5. ER stress promotes I/R-induced cardiomyocyte pyroptosis and cardiac function injury in mice. The nude mice were treated with TM, PBS, 4-PBA combined with I/R or I/R alone. A, the mRNA expression of Calpain, NLRP3, GRP78 and CHOP; B–C, the protein expression of Calpain, NLRP3, GRP78 and CHOP; D–E, the PI/Hoechst 33342 double staining results of the cardiomyocyte pyroptosis (200×); F, the ultrastructure of cardiomyocyte tissues in each group (scale bar = 500 nm) under an TEM; G–H, the myocardial infarct size in each group tested by TTC/Evans blue staining; the measurement data were expressed with the mean ± standard deviation; difference among groups was compared by one-way analysis of variance, followed by Tuckey's post hoc test; in panels A and C, n = 3, in panel H, n = 4, and other experiments were conducted 3 times; *, $p < 0.05$ vs. the I/R group.

factor in the si-NC + I/R group ($p > 0.05$), while the expression of NLRP3, ASC, Caspase-1, GRP78 and CHOP was remarkably decreased in the si-NLRP3 + I/R group ($p < 0.05$; Fig. 7A–C).

Pyroptosis rate was detected and the results showed that compared with the I/R group, there was no significant difference in the cardiomyocyte pyroptosis rate of the si-NC + I/R group ($p > 0.05$); in the si-NLRP3 + I/R group, the cardiomyocyte pyroptosis rate was significantly decreased ($p < 0.05$). The results from TEM and TTC/Evans blue staining revealed that there was no significant difference in the cell ultrastructure and myocardial infarction size in mice of the si-NC + I/R group in comparison to those of the I/R group ($p > 0.05$). In the si-NLRP3 + I/R group, the cardiomyocyte injury was reduced, the ER was not dilated, the mitochondria appeared to have occasional vacuolization, and there was a significant reduction in the myocardial infarction size (all $p < 0.05$; Fig. 7D–H). The myocardial function detection results showed that compared with the I/R group, there was no significant difference in the cardiac function indexes of the si-NC + I/R group ($p > 0.05$); in the si-NLRP3 + I/R group, the LVEDP value in mice was significantly decreased ($p < 0.05$), while the LVSP, HR, CF, $+dp/dt_{max}$, $-dp/dt_{max}$ values in mice were significantly increased

Table 3
The myocardiac function indexes of mice in each group.

Group	LVSP (mmHg)	LVDEP (mmHg)	$+dp/dt_{max}$ (mmHg/s)	$-dp/dt_{max}$ (mmHg/s)	HR (times/min)	CF (mL/min)
I/R	92.15 ± 8.26	11.38 ± 2.54	3572.84 ± 554.28	3418.46 ± 547.26	276.67 ± 20.31	3.57 ± 0.43
PBS + I/R	89.47 ± 7.82	12.52 ± 1.36	3350.47 ± 531.19	3306.88 ± 518.76	289.33 ± 18.50	3.42 ± 0.38
TM + I/R	63.45 ± 7.21*	18.95 ± 2.62*	2484.56 ± 512.47*	2348.19 ± 521.17*	202.00 ± 15.62*	1.27 ± 0.23*
4-PBA + I/R	126.18 ± 9.52*	5.08 ± 0.87*	4598.59 ± 608.88*	4542.58 ± 545.38*	351.67 ± 25.42*	6.57 ± 0.86*

Notes: LVSP, left ventricular systolic pressure; LVDEP, left ventricular end diastolic pressure; $+dp/dt_{max}$, the maximal rate of rise of the left ventricular pressure; $-dp/dt_{max}$, the maximal rate of fall of the left ventricular pressure; HR, heart rate; CF, coronary flow; PBS, phosphate buffer solution; I/R, Ischemia-reperfusion; TM, tunicamycin; 4-PBA, 4-phenyl butyric acid. The measurement data (data in table) were expressed with the mean ± standard deviation; difference among groups was compared by one-way analysis of variance, followed by Turkeys' post hoc test, n = 3.

* $p < 0.05$ vs. the I/R group.

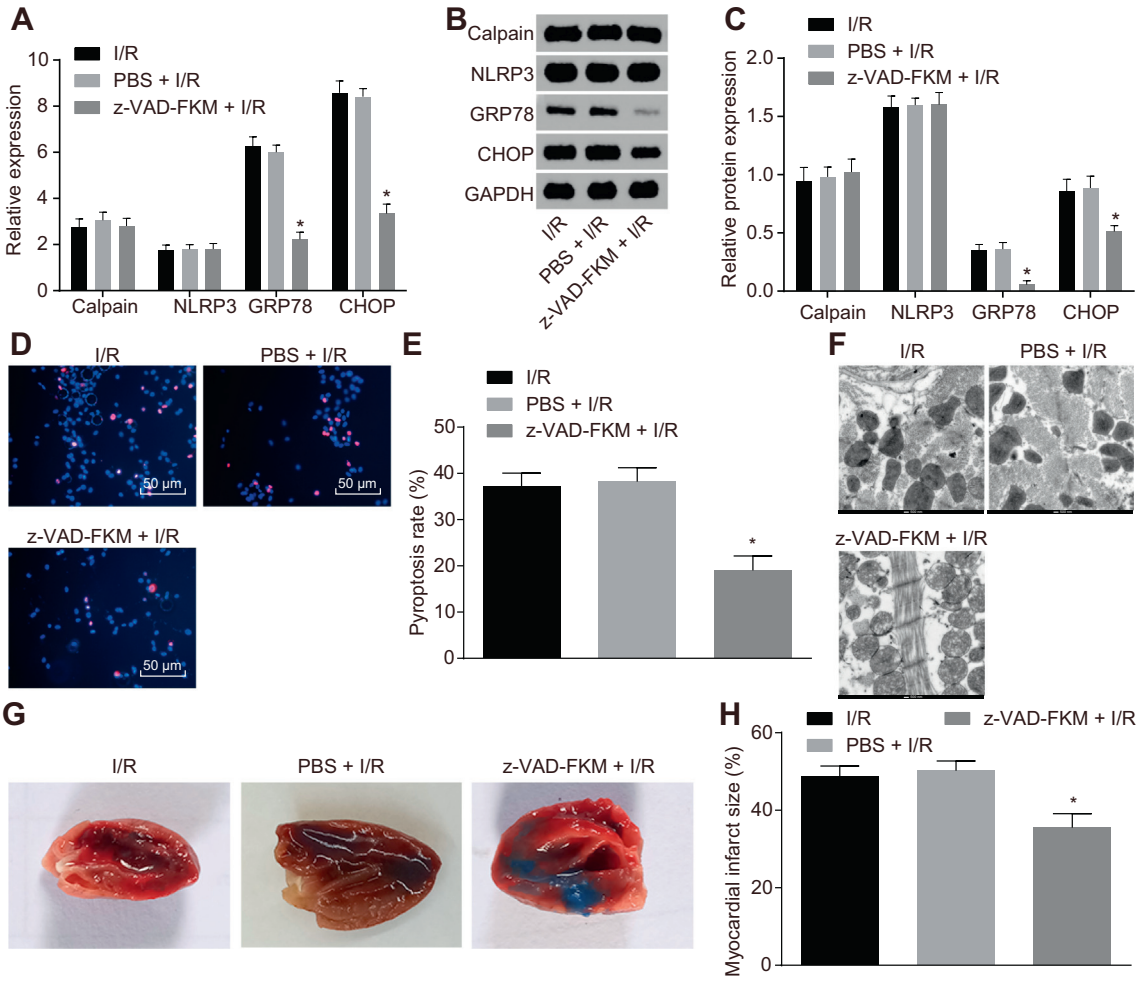

Fig. 6. Caspase-1 promotes I/R-induced cardiomyocyte pyroptosis and cardiac function injury in I/R mice. The nude mice were treated with PBS, z-VAD-FKM combined with I/R or I/R alone. A, the mRNA expression of Calpain, NLRP3, GRP78, CHOP; B–C, the protein expression of Calpain, NLRP3, GRP78, CHOP, GAPDH; C, the protein level of Calpain, NLRP3, GRP78, CHOP, GAPDH after alteration of Caspase-1; D–E the PI/Hoechst 33342 double staining results of cardiomyocyte pyroptosis after alteration of Caspase-1 (200 ×); F, the ultrastructure of cardiomyocyte tissues after alteration of Caspase-1 (scale bar = 500 nm) under an TEM; G-H, the myocardial infarct size after alteration of Caspase-1 tested by TTC/Evans blue staining; the measurement data were expressed with the mean ± standard deviation; difference among groups was compared by one-way analysis of variance; in panels A and C, n = 3, in panel H, n = 4, and other experiments were conducted 3 times, followed by Tuckey's post hoc test; *, $p < 0.05$ vs. the I/R group.

($p < 0.05$; Table 5). These findings suggest that NLRP3 could potentially induce cardiomyocyte pyroptosis, and further promote myocardial infarction and cardiac function injury in mice.

3.10. Calpain induces cardiomyocyte pyroptosis and further promotes myocardial infarction and cardiac function injury in I/R mice

The effect of Calpain on myocardial function in I/R mice was further investigated by interfering with and overexpressing Calpain. Based on the results from the RT-qPCR and western blot analysis, there was no significant difference observed in the expression of Calpain, NLRP3, ASC, Caspase-1, GRP78 and CHOP in the pcDNA control + I/R group in comparison with the I/R group ($p > 0.05$); the expression of these factor in the pcDNA Calpain + I/R group was significantly increased ($p < 0.05$); where opposite trends were observed in the si-Calpain + I/R group ($p < 0.05$). Calpain activity was detected and the results revealed that compared with the I/R group, there was no significant difference in Calpain activity in the pcDNA control + I/R group

Table 4
The myocardiac function indexes of mice after overexpression of caspase-1.

Group	LVSP (mmHg)	LVDEP (mmHg)	$+dp/dt_{max}$ (mmHg/s)	$-dp/dt_{max}$ (mmHg/s)	HR (times/min)	CF (mL/min)
I/R	92.15 ± 8.26	11.38 ± 2.54	3572.84 ± 554.28	3418.46 ± 547.26	276.67 ± 20.31	3.57 ± 0.43
PBS + I/R	89.47 ± 7.82	10.52 ± 2.36	3350.47 ± 531.19	3306.88 ± 518.76	289.33 ± 18.50	3.42 ± 0.38
z-VAD-FKM + I/R	108.65 ± 9.52*	5.52 ± 1.64*	4667.85 ± 621.44*	4584.19 ± 598.17*	372.33 ± 28.01*	5.87 ± 0.42*

Note: LVSP, left ventricular systolic pressure; LVDEP, left ventricular end diastolic pressure; $+dp/dt_{max}$, the maximal rate of rise of the left ventricular pressure; $-dp/dt_{max}$, the maximal rate of fall of the left ventricular pressure; HR, heart rate; CF, coronary blood flow; PBS, phosphate buffer solution; I/R, Ischemia-reperfusion. The measurement data (data in table) were expressed with the mean ± standard deviation. Difference among groups were compared by one-way analysis of variance, followed by Turkeys' post hoc test, n = 3.

* $p < 0.05$ vs. the I/R group.

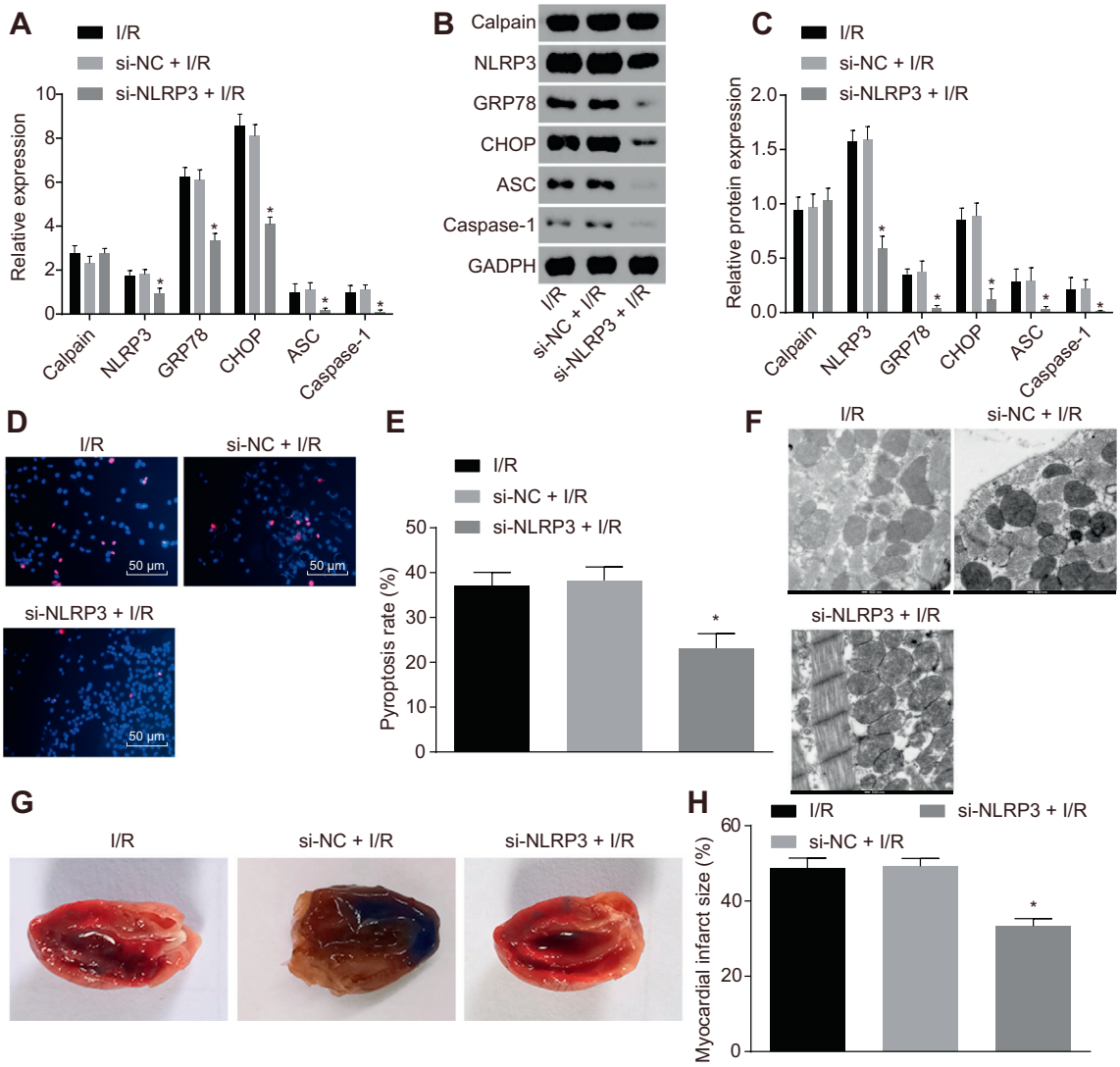

Fig. 7. NLRP3 promotes I/R-induced cardiomyocyte pyroptosis and cardiac function injury in I/R mice. The nude mice were treated with si-NC, si-NLRP3 combined with I/R or I/R alone. A, the mRNA expression of Calpain, NLRP3, GRP78, CHOP, ASC, Caspase-1; B–C, the protein expression of Calpain, NLRP3, ASC, GRP78, CHOP, GAPDH, Caspase-1; D–E, the PI/Hoechst 33342 double staining results of cardiomyocyte pyroptosis (200×); F, the ultrastructure of cardiomyocyte tissues after alteration of NLRP3 (scale bar = 500 nm) under an TEM; G–H, the myocardial infarct size tested by TTC/Evans blue staining; the measurement data were expressed with the mean ± standard deviation; difference among groups was compared by one-way analysis of variance; in panels A and C, n = 3, in panel H, n = 4, and other experiments were conducted 3 times, followed by Tuckey's post hoc test; *, $p < 0.05$ vs. the I/R group.

Table 5
The myocardiac function indexes of mice after silencing of NLRP3.

Group	LVSP (mmHg)	LVDEP (mmHg)	$+dp/dt_{max}$ (mmHg/s)	$-dp/dt_{max}$ (mmHg/s)	HR (times/min)	CF (mL/min)
I/R	92.15 ± 8.26	11.38 ± 2.54	3572.84 ± 554.28	3418.46 ± 547.26	276.67 ± 20.31	3.57 ± 0.43
si-NC + I/R	88.21 ± 7.37	10.65 ± 2.39	3356.69 ± 532.23	3285.42 ± 514.11	271.33 ± 17.50	3.52 ± 0.36
si-NLRP3 + I/R	108.65 ± 8.71*	5.21 ± 1.56*	4604.71 ± 609.92*	4521.04 ± 586.65*	392.33 ± 35.57*	5.76 ± 0.62*

Notes: LVSP, left ventricular systolic pressure; LVDEP, left ventricular end diastolic pressure; $+dp/dt_{max}$, the maximal rate of rise of the left ventricular pressure; $-dp/dt_{max}$, the maximal rate of fall of the left ventricular pressure; HR, heart rate; CF, coronary blood flow; NLRP3, NLR pyrin domain containing 3; I/R, Ischemia-reperfusion. The measurement data (data in table) were expressed with the mean ± standard deviation; difference among groups was compared by one-way analysis of variance, followed by Turkeys' post hoc test, n = 3.

* $p < 0.05$ vs. the I/R group.

($p > 0.05$); Calpain activity in the pcDNA Calpain + I/R group was significantly increased, while Calpain activity in the si-Calpain + I/R group was significantly decreased (all $p < 0.05$; Fig. 8A–D).

The detection of the pyroptosis rate showed that compared with the pcDNA control + I/R group, pyroptosis rate was significantly increased in the pcDNA Calpain + I/R, pcDNA Calpain + z-VAD-FKM + I/R, pcDNA Calpain + si-NLRP3 + I/R and pcDNA Calpain + 4-PBA + I/R groups, with the most evident increase observed in the pcDNA Calpain + I/R group (all $p < 0.05$), while pyroptosis rate was significantly decreased in the si-Calpain + I/R group ($p < 0.05$). The results from TEM and TTC/Evans blue staining showed that compared with the pcDNA control + I/R group, the degree of myocardium injury and the

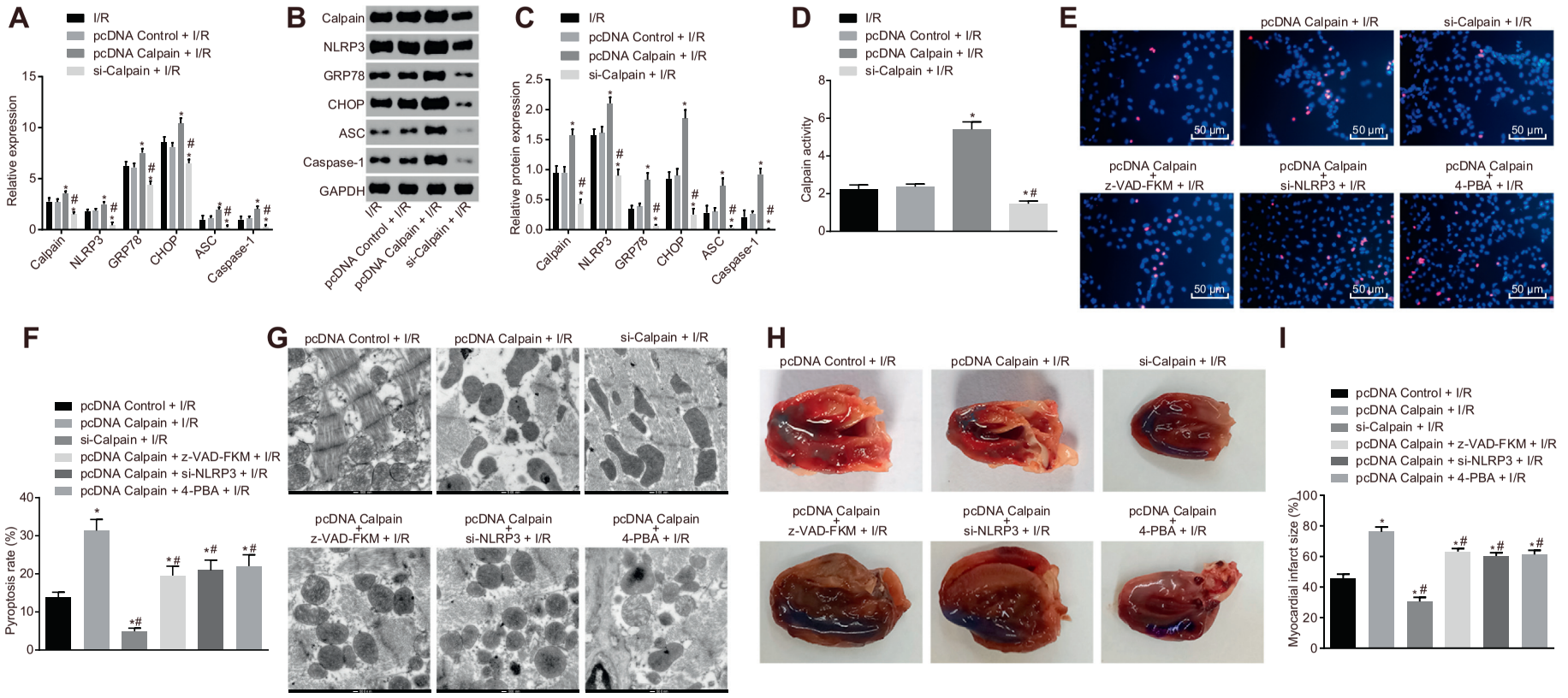

Fig. 8. Calpain expression promotes I/R-induced cardiomyocyte pyroptosis and cardiac function injury in I/R mice. The nude mice were treated with pcDNA Control, pcDNA Calpain or si-Calpain combined with I/R or I/R alone. A, the mRNA expression of Calpain, NLRP3, GRP78, CHOP, ASC, Caspase-1; B–C, the protein expression of Calpain, NLRP3, ASC, GRP78, CHOP, GAPDH, Caspase-1; D, the Calpain activity; The nude mice were treated with pcDNA Control, pcDNA Calpain, si-Calpain, pcDNA Calpain plus z-VAD-FKM, si-NLRP3, or 4-PBA in combined with I/R. E–F, the PI/Hoechst 33342 double staining results of cardiomyocyte pyroptosis (200×); G, the ultrastructure of cardiomyocyte tissues (scale bar = 500 nm) under an TEM; H–I, the myocardial infarct tested by TTC/Evans blue staining size; the measurement data were expressed with the mean ± standard deviation; difference among groups was compared by one-way analysis of variance; in panels A and C, n = 3, in panel I, n = 4, and other experiments were conducted 3 times, followed by Tuckey's post hoc test; *, $p < 0.05$ vs. the I/R group or pcDNA control + I/R group; #, $p < 0.05$ vs. the pcDNA Calpain + I/R group.

Table 6
The myocardiac function indexes of mice after alteration of caspase-1, NLRP3 and Calpain.

Group	LVSP (mmHg)	LVDEP (mmHg)	$+dp/dt_{max}$ (mmHg/s)	$-dp/dt_{max}$ (mmHg/s)	HR (times/min)	CF (mL/min)
pcDNA Control + I/R	92.64 ± 8.26	11.21 ± 2.12	3524.28 ± 562.47	3382.64 ± 547.26	315.33 ± 12.37	4.24 ± 0.49
pcDNA Calpain + I/R	45.28 ± 7.26*	29.88 ± 2.53*	1561.43 ± 482.55*	1358.41 ± 321.17*	145.00 ± 13.89*	2.51 ± 0.34*
si-Calpain + I/R	117.24 ± 9.24*	5.19 ± 1.22*	4682.46 ± 621.62*	4469.72 ± 598.47*	558.33 ± 19.60*	7.92 ± 0.80*
pcDNA Calpain + z-VAD-FKM + I/R	65.17 ± 7.18#	17.12 ± 2.07#	2601.17 ± 542.13#	2312.75 ± 525.63#	443.33 ± 15.50#	6.05 ± 0.42#
PcDNA Calpain + si-NLRP3 + I/R	63.57 ± 8.04#	18.92 ± 2.11#	2385.34 ± 561.12#	2412.75 ± 525.63#	435.67 ± 29.50#	6.76 ± 0.60#
pcDNA Calpain + 4-PBA + I/R	62.33 ± 7.96#	16.68 ± 1.65#	2616.43 ± 572.44#	2246.57 ± 538.16#	438.00 ± 11.79#	6.88 ± 0.67#

Notes: LVSP, left ventricular systolic pressure; LVDEP, left ventricular end diastolic pressure; $+dp/dt_{max}$, the maximal rate of rise of the left ventricular pressure; $-dp/dt_{max}$, the maximal rate of fall of the left ventricular pressure; HR, heart rate; CF, coronary flow; NLRP3, NLR pyrin domain containing 3; I/R, Ischemia-reperfusion; 4-PBA, 4-phenyl butyric acid. The measurement data (data in table) were expressed with the mean ± standard deviation; difference among groups was compared by one-way analysis of variance, followed by Turkeys' post hoc test, n = 3.

* $p < 0.05$ vs. the pcDNA control + I/R group.

# $p < 0.05$ vs. the pcDNA Calpain + I/R group.

myocardial infarction size were significantly increased in the pcDNA Calpain + I/R group, the pcDNA Calpain + z-VAD-FKM + I/R group, the pcDNA Calpain + si-NLRP3 + I/R group and the pcDNA Calpain + 4-PBA + I/R group, with the most serious myocardial injury and the largest myocardial infarction size observed in the pcDNA Calpain + I/R group ($p < 0.05$); the si-Calpain + I/R group presented with improved cardiomyocyte injury with no dilation in ER, occasional vacuolization in mitochondrion, and smallest myocardial infarction size ($p < 0.05$; Fig. 8E–I). The results from the detection of myocardial function revealed that compared with the pcDNA control + I/R group, the LVEDP value was significantly elevated in the pcDNA Calpain + I/R, pcDNA Calpain + z-VAD-FKM + I/R, Calpain + si-NLRP3 + I/R and pcDNA Calpain + 4-PBA + I/R groups ($p < 0.05$), while the LVSP, HR, CF, $+dp/dt_{max}$ and $-dp/dt_{max}$ values were significantly decreased, the pcDNA Calpain + I/R group presented with the most severe cardiac function injury (all $p < 0.05$); in the si-Calpain + I/R group, the LVEDP value was significantly decreased ($p < 0.05$), while the LVSP, HR, CF, $+dp/dt_{max}$, $-dp/dt_{max}$ values were significantly increased ($p < 0.05$; Table 6). These findings suggest that Calpain could induce cardiomyocyte pyroptosis in I/R-induced mice, and further promote myocardial infarction and cardiac function injury by mediating the NLRP3/ASC/Caspase-1 axis in order to activate ER stress, indicating that Calpain knockout might result in the alleviation of the aforementioned symptoms in I/R-induced mice.

4. Discussion

I/R injury, a multi-factor antigen-independent inflammatory disease, is confirmed by both clinical and experimental data to profoundly affect the early and long-term function of allotransplantation [26]. Previous studies have highlighted that Calpain activity regulates the activation of the ATP-driven NLRP3 inflammasome [27]. The inhibition of ER stress has also been reported to result in the significant alleviation of I/R injury in myocardium [28]. The present study subjected to H/R in cardiomyocytes to simulate I/R injury in mice, and the findings revealed that Calpain could promote the activation of NLRP3/ASC/Caspase-1 axis and the focal death and injury of cardiac cells caused by H/R. In addition, our findings also provided evidence that NLRP3/ASC/Caspase-1 axis could increase the infarct size and cardiac function injury of I/R-induced mice.

Based on evidence provided by the present study, H/R has been proven to promote Calpain activation and ER stress in cardiomyocytes, and induce cardiomyocyte pyroptosis. The close relationship between cardiovascular diseases including myocardial infarction, hypertrophy and heart failure and ER stress has been evidently demonstrated in previous studies [29]. This present study found a significant increase in the cardiomyocyte pyroptosis rate and larger myocardial infarct size in the I/R-induced mice. Moreover, the cardiac function indexes of LVEDP were significantly elevated, while the LVSP, HR, CF, $+dp/dt_{max}$, and $-dp/dt_{max}$ showed the opposite trend in the I/R-induced mice. However , the inhibition of ER stress/NLRP3/Caspase-1/Calpain has been found to result in the reduction of cardiomyocyte pyroptosis rate and myocardial infarct size; the LVEDP value was significantly decreased, while the LVSP, HR, CF $+dp/dt_{max}$, and $-dp/dt_{max}$ values were on the contrary with ER stress/NLRP3/Caspase-1/Calpain inhibition. Myocardial infarction could induce an intense inflammatory response, which is another unfavorable condition for cardiac repair [30]. The ER stress-induced apoptotic pathway has been reported to be closely correlated with the development of acute myocardial infarction processing, and the inhibition of ER stress-induced apoptosis could provide protection for the heart against cardiomyocyte loss and improve cardiac function [31]. Another study has also mentioned that in comparison with the model rats with cardiomyopathy, the HR, LVSP, $+dp/dt_{max}$, and $-dp/dt_{max}$ were decreased, while the LVEDP was increased following moxibustion intervention in the rats, indicating grain-moxibustion could potentially lead to the improvement of left ventricular function and increase HR in cardiomyopathy rats [32].

The findings from the present study demonstrated that NLRP3/ASC/Caspase-1 axis could lead to the increase of infarct size and myocardial function injury in I/R-induced mice. ASC interacts with NLRP3 accompanied by pro-Caspase-1 within the inflammasome complex which subsequently results in the activation of Caspase-1 [33]. In addition, it has been investigated that pyroptosis, a specific type of cell death, was independently activated by Caspase-1 activity [34], which is characterized by rapid death and the facilitation of pathogen clearance as a result of the infection of the macrophages with intracellular pathogens [8]. The activation of NLRP3 inflammasome has been demonstrated to induce hepatocyte pyroptosis and other symptoms, including liver inflammation and fibrosis [35]. Moreover, in the diabetic rats, hyperglycaemia-induced NLRP3 inflammasome activation could activate ROS-dependent process causing pyroptosis, and the NLRP3 inflammasome-induced pyroptosis could also result in an increase in myocardial I/R injury [36].

Furthermore, Calpain could promote the activation of NLRP3/ASC/Caspase-1 axis, and the focal death and injury of cardiac cells caused by H/R, while the knockout of Calpain gene could inhibit ER stress of the mice in vivo, and reduce the myocardial infarct size and myocardial function injury in mice that had received treatment for I/R. Another study has reported that the inhibition of NLRP3-inflammasome could lead to a decrease in myocardial infarction and improve myocardial function, which was demonstrated in animal myocardial infarction models [37]. The mediation of a Caspase inhibitor (zVAD) led to the improvement of myocardial Caspase-3 activity and cardiac physiologic function control, suggesting its physiologic role in lipopolysaccharide-induced cardiac dysfunction [38]. The presence of ASC in myocardial infarction of human myocardial tissues has been clearly observed in a previous study [10]. It has previously been reported that the Caspase-1 inhibitor VX-765 combined with a platelet inhibitor provides protection

against myocardial infarction in the mice [39]. Following the post-ischemic administration of Caspase-l inhibitor of Ac-YVAD-cmk, the infarction size was markedly decreased in a rabbit experiment [40]. Calpains, as a group of calcium-dependent proteases, are excessively activated in several kinds of pathological conditions due to an increase in endocellular calcium levels [41]. Calpain-2 inhibition or knockdown could promote autophagy and inhibit cell death [42], which was consistent with our findings. Moreover, the suppression of myocardial infarction-induced Calpain activation in mice by calpeptin (an aldehydic inhibitor of Calpain) treatment has been reported to provide protection for cardiomyocytes of mice against myocardial cell loss, while improving ventricular function [43], indicating that the inhibition of Calpain activity could prevent structural and functional injury of myocardial cells in later stages of myocardial infarction during I/R [17]. H/R could potentially promote the activity of Calpain and the expression of NLRP3 in cardiomyocytes, thereby facilitating ER stress and cardiomyocyte pyroptosis. Following the inhibition of Calpain expression and the NLRP3/ASC/Caspase-1 pathway axis, cardiomyocyte pyroptosis was suppressed. Our results suggested that Calpain induced NLRP3/ASC/Caspase-1 axis and ER stress, thus potentiating cardiomyocyte pyroptosis. These in vitro findings were also reproduced in vivo on I/R mice.

5. Conclusion

In conclusion, the findings from our study were indicative of the promoting effect of I/R on cardiomyocyte pyroptosis and myocardial dysfunction in mice based on the prior experiments. The inhibition or knockout of Calpain could also regulate the activation of ER stress and further reduce pyroptosis through the NLRP3/ASC/Caspase-1 axis in I/R-induced mice. These findings suggest that Calpain could be a promising therapeutic pathway for I/R injury, which is of great importance to improve the treatment and prognosis of I/R injury. However, the present study did not thoroughly investigate the relationship between Calpain inhibitor and the NLRP3/ASC/Caspase-1 axis. Therefore, further research is required to provide additional insight on this subject. We also believe that the effects of calpain overexpression on mitochondrial structure, whether any interleukin or inflammation arising from macrophage infiltration or whether the signaling kinases such as AKT or AMPK are involved in H/R or I/R injury should all be further investigated in order to provide supportive data for our findings.

Supplementary data to this article can be found online at https://doi.org/10.1016/j.lfs.2019.116631.

Funding

This work was supported by the National Natural Science Foundation of China (81600232), Science and Technology Strategic Special Cooperation between City and University in NanChong (18SXHZ0458; NSMC20170210), Key Projects of Education Department of Sichuan Province (17ZA0183) and North Sichuan Medical College Doctoral Research Initial Fund (CBY15-QD12).

Authors' contributions

Rong-Chuan Yue, Sheng-Zhong Lu and Yu Luo designed the study. Tao Wang, Hao Liang and Jing Zeng collated the data, carried out data analyses and produced the initial draft of the manuscript. Jie Liu and Hou-Xiang Hu contributed to drafting and polishing the manuscript. All authors have read and approved the final submitted manuscript.

Declaration of Competing Interest

The authors declare no conflict of interest.

Acknowledgements

We acknowledge and appreciate our colleagues for their valuable efforts and comments on this paper.

References

[1] T. Kalogeris, C.P. Baines, M. Krenz, et al., Cell biology of ischemia/reperfusion injury, Int. Rev. Cell Mol. Biol. 298 (2012) 229–317.
[2] V. Sala, T. Crepaldi, Novel therapy for myocardial infarction: can HGF/Met be beneficial? Cell. Mol. Life Sci. 68 (10) (2011) 1703–1717.
[3] Y.T. Liu, H.M. Jia, X. Chang, et al., The metabolic disturbances of isoproterenol induced myocardial infarction in rats based on a tissue targeted metabonomics, Mol. BioSyst. 9 (11) (2013) 2823–2834.
[4] T. Bergsbaken, S.L. Fink, B.T. Cookson, Pyroptosis: host cell death and inflammation, Nat. Rev. Microbiol. 7 (2) (2009) 99–109.
[5] L. Jian, Y. Lu, S. Lu, et al., Chemical chaperone 4-phenylbutyric acid protects H9c2 cardiomyocytes from ischemia/reperfusion injury by attenuating endoplasmic reticulum stress-induced apoptosis, Mol. Med. Rep. 13 (5) (2016) 4386–4392.
[6] M.A. Reichenberger, S. Heimer, A. Schaefer, et al., Adipose derived stem cells protect skin flaps against ischemia-reperfusion injury, Stem Cell Rev. 8 (3) (2012) 854–862.
[7] J. Thompson, Y. Hu, E.J. Lesnefsky, et al., Activation of mitochondrial calpain and increased cardiac injury: beyond AIF release, Am. J. Physiol. Heart Circ. Physiol. 310 (3) (2016) H376–H384.
[8] E.A. Miao, I.A. Leaf, P.M. Treuting, et al., Caspase-1-induced pyroptosis is an innate immune effector mechanism against intracellular bacteria, Nat. Immunol. 11 (12) (2010) 1136–1142.
[9] Y. Liu, K. Lian, L. Zhang, et al., TXNIP mediates NLRP3 inflammasome activation in cardiac microvascular endothelial cells as a novel mechanism in myocardial ischemia/reperfusion injury, Basic Res. Cardiol. 109 (5) (2014) 415.
[10] M. Kawaguchi, M. Takahashi, T. Hata, et al., Inflammasome activation of cardiac fibroblasts is essential for myocardial ischemia/reperfusion injury, Circulation 123 (6) (2011) 594–604.
[11] M. Kitazawa, S. Hida, C. Fujii, et al., ASC induces apoptosis via activation of caspase-9 by enhancing gap junction-mediated intercellular communication, PLoS One 12 (1) (2017) e0169340.
[12] X. Li, F. Zhong, Nickel induces interleukin-1beta secretion via the NLRP3-ASC-caspase-1 pathway, Inflammation 37 (2) (2014) 457–466.
[13] H. Huang, H.W. Chen, J. Evankovich, et al., Histones activate the NLRP3 inflammasome in Kupffer cells during sterile inflammatory liver injury, J. Immunol. 191 (5) (2013) 2665–2679.
[14] Y. Kaneko, C.R. Murphy, M.L. Day, Calpain 2 activity increases at the time of implantation in rat uterine luminal epithelial cells and administration of calpain inhibitor significantly reduces implantation sites, Histochem. Cell Biol. 141 (4) (2014) 423–430.
[15] Y. Yang, W. Duan, J. Zhou, et al., Protective effects of adenosine on the diabetic myocardium against ischemia-reperfusion injury: role of calpain, Med. Hypotheses 79 (4) (2012) 462–464.
[16] V. Hernando, J. Inserte, C.L. Sartorio, et al., Calpain translocation and activation as pharmacological targets during myocardial ischemia/reperfusion, J. Mol. Cell. Cardiol. 49 (2) (2010) 271–279.
[17] C. Neuhof, H. Neuhof, Calpain system and its involvement in myocardial ischemia and reperfusion injury, World J. Cardiol. 6 (7) (2014) 638–652.
[18] X. Yang, R. Yue, J. Zhang, et al., Gastrin protects against myocardial ischemia/reperfusion injury via activation of RISK (reperfusion injury salvage kinase) and SAFE (survivor activating factor enhancement) pathways, J. Am. Heart Assoc. 7 (14) (2018).
[19] S. Liu, N. Wu, J. Miao, et al., Protective effect of morin on myocardial ischemiareperfusion injury in rats, Int. J. Mol. Med. 42 (3) (2018) 1379–1390.
[20] S. Bansal, G. Biswas, N.G. Avadhani, Mitochondria-targeted heme oxygenase-1 induces oxidative stress and mitochondrial dysfunction in macrophages, kidney fibroblasts and in chronic alcohol hepatotoxicity, Redox Biol. 2 (2014) 273–283.
[21] D. Liu, Effects of procyanidin on cardiomyocyte apoptosis after myocardial ischemia reperfusion in rats, BMC Cardiovasc. Disord. 18 (1) (2018) 35.
[22] V. Kohli, W. Gao, C.A. Camargo Jr.et al., Calpain is a mediator of preservation-reperfusion injury in rat liver transplantation, Proc. Natl. Acad. Sci. U. S. A. 94 (17) (1997) 9354–9359.
[23] T. Luo, R. Yue, H. Hu, et al., PD150606 protects against ischemia/reperfusion injury by preventing mu-calpain-induced mitochondrial apoptosis, Arch. Biochem. Biophys. 586 (2015) 1–9.
[24] R. Yue, H. Hu, K.H. Yiu, et al., Lycopene protects against hypoxia/reoxygenation-induced apoptosis by preventing mitochondrial dysfunction in primary neonatal mouse cardiomyocytes, PLoS One 7 (11) (2012) e50778.
[25] S. Wang, F. Zhang, G. Zhao, et al., Mitochondrial PKC-epsilon deficiency promotes I/R-mediated myocardial injury via GSK3beta-dependent mitochondrial permeability transition pore opening, J. Cell. Mol. Med. 21 (9) (2017) 2009–2021.
[26] P. Boros, J.S. Bromberg, New cellular and molecular immune pathways in ischemia/reperfusion injury, Am. J. Transplant. 6 (4) (2006) 652–658.
[27] E. Valimaki, W. Cypryk, J. Virkanen, et al., Calpain activity is essential for ATP-driven unconventional vesicle-mediated protein secretion and inflammasome activation in human macrophages, J. Immunol. 197 (8) (2016) 3315–3325.
[28] F. Yuan, L. Zhang, Y.Q. Li, et al., Chronic intermittent hypobaric hypoxia improves cardiac function through inhibition of endoplasmic reticulum stress, Sci. Rep. 7 (1)

(2017) 7922.
[29] Y. Xu, L. Wu, A. Chen, et al., Protective effects of olive leaf extract on acrolein-exacerbated myocardial infarction via an endoplasmic reticulum stress pathway, Int. J. Mol. Sci. 19 (2) (2018).
[30] K. Yang, C. Xu, Y. Zhang, et al., Sestrin2 suppresses classically activated macrophages-mediated inflammatory response in myocardial infarction through inhibition of mTORC1 signaling, Front. Immunol. 8 (2017) 728.
[31] Z.Y. Shi, Y. Liu, L. Dong, et al., Cortistatin improves cardiac function after acute myocardial infarction in rats by suppressing myocardial apoptosis and endoplasmic reticulum stress, J. Cardiovasc. Pharmacol. Ther. (2016), https://doi.org/10.1177/1074248416644988.
[32] Y. Xiao, L. Ding, H. Chen, et al., Grain-moxibustion may protect myocardium by reducing oxidative stress in doxorubicin-induced cardiomyopathy rats, Zhen Ci Yan Jiu 41 (6) (2016) 502–508.
[33] V. Compan, F. Martin-Sanchez, A. Baroja-Mazo, et al., Apoptosis-associated speck-like protein containing a CARD forms specks but does not activate caspase-1 in the absence of NLRP3 during macrophage swelling, J. Immunol. 194 (3) (2015) 1261–1273.
[34] K. Motani, H. Kushiyama, R. Imamura, et al., Caspase-1 protein induces apoptosis-associated speck-like protein containing a caspase recruitment domain (ASC)-mediated necrosis independently of its catalytic activity, J. Biol. Chem. 286 (39) (2011) 33963–33972.
[35] A. Wree, A. Eguchi, M.D. McGeough, et al., NLRP3 inflammasome activation results in hepatocyte pyroptosis, liver inflammation, and fibrosis in mice, Hepatology 59 (3) (2014) 898–910.
[36] Z. Qiu, S. Lei, B. Zhao, et al., NLRP3 inflammasome activation-mediated pyroptosis aggravates myocardial ischemia/reperfusion injury in diabetic rats, Oxidative Med. Cell. Longev. 2017 (2017) 9743280.
[37] G.P. van Hout, L. Bosch, G.H. Ellenbroek, et al., The selective NLRP3-inflammasome inhibitor MCC950 reduces infarct size and preserves cardiac function in a pig model of myocardial infarction, Eur. Heart J. 38 (11) (2017) 828–836.
[38] D.L. Carlson, M.S. Willis, D.J. White, et al., Tumor necrosis factor-alpha-induced caspase activation mediates endotoxin-related cardiac dysfunction, Crit. Care Med. 33 (5) (2005) 1021–1028.
[39] X.M. Yang, J.M. Downey, M.V. Cohen, et al., The highly selective caspase-1 inhibitor VX-765 provides additive protection against myocardial infarction in rat hearts when combined with a platelet inhibitor, J. Cardiovasc. Pharmacol. Ther. 22 (6) (2017) 574–578.
[40] T.D. Wang, W.J. Chen, T.J. Mau, et al., Attenuation of increased myocardial ischaemia-reperfusion injury conferred by hypercholesterolaemia through pharmacological inhibition of the caspase-1 cascade, Br. J. Pharmacol. 138 (2) (2003) 291–300.
[41] S.Y. Cheng, S.C. Wang, M. Lei, et al., Regulatory role of calpain in neuronal death, Neural Regen. Res. 13 (3) (2018) 556–562.
[42] Q. Zhao, Z. Guo, W. Deng, et al., Calpain 2-mediated autophagy defect increases susceptibility of fatty livers to ischemia-reperfusion injury, Cell Death Dis. 7 (2016) e2186.
[43] S.K. Mani, S. Balasubramanian, J.A. Zavadzkas, et al., Calpain inhibition preserves myocardial structure and function following myocardial infarction, Am. J. Physiol. Heart Circ. Physiol. 297 (5) (2009) H1744–H1751.